ARMY RESEARCH LABORATORY

Tensile Properties of Dyneema SK76 Single Fibers at Multiple Loading Rates Using a Direct Gripping Method

by Brett Sanborn, Ann Mae DiLeonardi, and Tusit Weerasooriya

ARL-TR-6974 **June 2014**

NOTICES

Disclaimers

The findings in this report are not to be construed as an official Department of the Army position unless so designated by other authorized documents.

Citation of manufacturer's or trade names does not constitute an official endorsement or approval of the use thereof.

Destroy this report when it is no longer needed. Do not return it to the originator.

Army Research Laboratory
Aberdeen Proving Ground, MD 21005-5069

ARL-TR-6974 **June 2014**

Tensile Properties of Dyneema SK76 Single Fibers at Multiple Loading Rates Using a Direct Gripping Method

Brett Sanborn
Oak Ridge Institute for Science and Education

Ann Mae DiLeonardi and Tusit Weerasooriya
Weapons and Materials Research Directorate, ARL

REPORT DOCUMENTATION PAGE	Form Approved OMB No. 0704-0188

1. REPORT DATE *(DD-MM-YYYY)*	2. REPORT TYPE	3. DATES COVERED (From - To)
June 2014	Final	1 April 2013–30 April 2014

4. TITLE AND SUBTITLE
Tensile Properties of Dyneema SK76 Single Fibers at Multiple Loading Rates Using a Direct Gripping Method

5a. CONTRACT NUMBER
1120-1120-99

5b. GRANT NUMBER

5c. PROGRAM ELEMENT NUMBER

6. AUTHOR(S)
Brett Sanborn, Ann Mae DiLeonardi, and Tusit Weerasooriya

5d. PROJECT NUMBER

5e. TASK NUMBER

5f. WORK UNIT NUMBER

7. PERFORMING ORGANIZATION NAME(S) AND ADDRESS(ES)
U.S. Army Research Laboratory
ATTN: RDRL-WMP-B
Aberdeen Proving Ground, MD 21005-5069

8. PERFORMING ORGANIZATION REPORT NUMBER
ARL-TR-6974

9. SPONSORING/MONITORING AGENCY NAME(S) AND ADDRESS(ES)

10. SPONSOR/MONITOR'S ACRONYM(S)

11. SPONSOR/MONITOR'S REPORT NUMBER(S)

12. DISTRIBUTION/AVAILABILITY STATEMENT
Approved for public release; distribution is unlimited.

13. SUPPLEMENTARY NOTES

14. ABSTRACT
Ultra-high-molecular-weight polyethylene (UHMWPE) fibers such as Dyneema and Spectra are seeing more use in lightweight armor applications due to higher tensile strength and lower density compared with aramid fibers such as Kevlar and Twaron. Numerical modeling is used to design more effective fiber-based composite armor. For accurate simulation of ballistic impacts, material response such as tensile stress-strain of the composite constituents must be studied under experimental conditions similar to ballistic events. UHMWPE fibers are difficult to grip using adhesive methods typically used for other fibers due to low surface energy. Based on previous studies, the ability to grip UHMWPE fibers using traditional adhesive methods depends on fiber diameter and is limited to smaller-diameter fibers that could affect reported stress values. To avoid diameter restrictions and surface energy problems, a direct gripping method has been used to characterize Dyneema SK76 single fibers at strain rates of 0.001 s^{-1}, 1 s^{-1}, and 1000 s^{-1}. In this report, the dependence of fiber diameter and gage length on failure strength is discussed as well as success rate of failures in the gage section with this gripping technique. A comparison of the tensile properties with previous studies is also explored.

15. SUBJECT TERMS
UHMWPE, Dyneema, SK76, fiber-based composite armor, strain rate

16. SECURITY CLASSIFICATION OF:			17. LIMITATION OF ABSTRACT	18. NUMBER OF PAGES	19a. NAME OF RESPONSIBLE PERSON
a. REPORT	b. ABSTRACT	c. THIS PAGE			Brett Sanborn
Unclassified	Unclassified	Unclassified	UU	30	19b. TELEPHONE NUMBER (*Include area code*) 410-306-4925

Standard Form 298 (Rev. 8/98)
Prescribed by ANSI Std. Z39.18

Contents

List of Figures

List of Tables

Acknowledgments

Thanks to Nicole Racine for her help in measuring fibers and doing experiments.

INTENTIONALLY LEFT BLANK.

1. Introduction

Aramid fibers such as Kevlar (DuPont) and Twaron (AZCO, The Netherlands) are frequently used in protective armor, though ultra-high-molecular-weight polyethylene (UHMWPE) fibers such as Dyneema (DSM Dyneema LLC) and Spectra (Honeywell) are more desirable due to lower density (0.97 g/cm^3) than aramids (1.44 g/cm^3). UHMWPE fibers also exhibit higher tensile modulus and good resistance to chemical and physical degradation. Due to an increasing need for numerical modeling capability of different soft armor systems, constituent-level material properties are required. Accurate simulation of impact events requires that material properties be collected under similar loading rate regimes and under valid experimental conditions. The primary loading mode on fibers used in protective equipment is axial tension; therefore, tensile experiments must be conducted at high strain rates that mimic loading rates seen in an impact event. UHMWPE fibers such as Dyneema and Spectra are notoriously difficult to grip for these tensile tests due to low surface energy (*1*), which has been reported by several authors (*2*, *3*).

The ability to grip Dyneema and other UHMWPE fibers using the standard gripping method for fibers, using an adhesive to attach the fibers to a cardboard substrate, depends on fiber diameter. Cochron et al. (*4*) studied Dyneema SK75 single fibers as part of a larger study on a nonwoven felt known as Dyneema Fraglight. After imaging fibers in a scanning electron microscope (SEM) and finding an average diameter of approximately 8 μm, the fibers were attached to cardboard substrates and successfully gripped and pulled in tension until failure in an Instron machine with a success rate of 75%. Hudspeth et al. (*5*) reinforce the diameter dependence on adhesive gripping Dyneema fibers using adhesives. In their study of the tensile properties of Dyneema SK76 single fiber with preapplied shear strain, Hudspeth et al. successfully used an adhesive method to pull 16-μm-diameter Dyneema fibers in tension.

Hybrid methods that include adhesives and mechanical gripping have been used by a few authors. Umberger (*2*) had gripping problems in his study on Spectra fibers that had an average diameter of 27.5 μm. Umberger settled on an adhesive method that also used cardboard mandrels by wrapping approximately 25 cm of fiber around each mandrel to obtain a 10-mm sample for tensile testing. Umberger acknowledged that this method was not ideal, as there was still slight slippage of the fiber as the fiber tightened around the mandrel as loading commenced. Russell et al. (*3*) had success performing quasi-static tensile tests on Dyneema SK76 single fibers that were glued to rubber end tabs using cyanoacrylate glue, followed by clamping in the serrated jaws of a screw-driven test machine. The authors of that report implied a low success rate using this gripping method, and showed a limited number of results.

Gripping methods that do not use adhesives have been used by others. Cansfield et al. (*6*) studied self-spun UHMWPE fiber at low strain rates using steel clamps and thin sheets of isotropic polyethylene to eliminate damage caused by the clamps. These self-spun UHMWPE fibers had strengths of 0.4–1.2 GPa, which are considerably weaker than Dyneema and Spectra fibers that fail at stresses of 2.9–4.0 GPa depending on the fiber type (*7*, *8*). Capstan-style grips that are typically used in yarn testing have also been used for UHMWPE single fibers (*9*). However, the exact gage length of specimens in capstan experiments is difficult to determine, which affects ultimate strain and measured modulus values.

Although adhesive-based methods have been shown to be effective for poly (p-phenylene terephthalamide) fibers (PPTA) (*10–13*), Kim et al. *(14–16*) have been developing a method of direct gripping on PPTA. This method includes directly clamping the fibers using poly methyl methacrylate blocks. The efficacy of this method to grip Kevlar fibers has been rigorously studied using a variety of statistical methods at different strain rates, including high strain rates that pose additional problems such as minimizing the overall grip size to fit on the Kolsky bar apparatus (*14–16*).

To overcome the difficulties associated with adhesive bonding, hybrid adhesive and mechanical methods, and mechanical methods alone that might not provide accurate strain measurements, a gripping method similar to that proposed by Kim et al. (*14–16*) has been altered and used in this investigation. With this novel gripping method we were able to collect accurate strain histories of single fiber samples and load specimens to failure without apparent fiber slippage from the gripping system. This technique is applicable to UHMWPE fibers over a large diameter range, and can be used at high strain rates. In addition to investigating the loading rate effects on SK76 fibers, a wide range of gage lengths was used to study the effect of defect distribution in the fiber.

2. Materials

Single fibers extracted from 1760-dtex* Dyneema SK76 yarns were used to study the uniaxial tensile behavior of Dyneema. Several samples were made from single fibers about 30 cm long that were glued to cardboard frames. Due to a high amount of variability in the diameter of Dyneema fiber, individual samples were imaged using an optical microscope with calibrated measuring software to record accurate diameter measurements. For each sample, about 10–20 measurements were taken at different locations along the fiber, averaged, and used as the fiber diameter in subsequent stress calculations. While some studies have suggested that UHMWPE fiber lacks roundness, and vibrometry methods are desirable to obtain cross-sectional area measurements (*9*), Russell et al. (*3*) showed that Dyneema SK76 single fibers were fairly circular

* dtex = mass in grams per 10,000 m.

in cross section. Vibrometry techniques are limited to samples longer than about 50 mm (*9*), which becomes problematic when trying to study the gage length dependence on tensile strength and the high-rate properties of fibers that require much shorter gage length samples (*5*, *10–13*).

For this report, the diameters of 73 single fibers 30 cm long were measured and used to make individual samples. Approximately 40–60 measurements were taken per fiber along the length. Some fibers showed a small variation of 0.296 μm (±1 standard deviation [SD]) along a 30-cm length, while other fibers had SDs as large as 1.67 μm along the length. The median diameter of 30-cm-long fibers used in this study was 18.12 ± 0.76 μm.

Since the diameter of the 30-cm-long fibers varied over the length, diameter measurements were taken for each individual sample for a total of 276 individual fiber samples. The average diameter of all 276 samples was 18.22 ± 1.15 μm, while the median diameter was 18.22 ± 0.46 μm. The largest diameter sample measured was 22.33 ± 1.14 μm, while the smallest diameter fiber sample was 14.53 ± 0.33 μm. The median SD in diameter over the collection of fiber samples was 0.46 μm, and the overall average SD was 0.53 μm.

Fibers of multiple gage lengths were used to study defect distribution. Quasi-static and intermediate rate experiments were conducted on specimens with gage lengths of 5, 10, and 50 mm. At high strain rates, specimens with gage lengths of 5, 7, and 10 mm were studied. Ten experiments were conducted at each gage length and strain rate for a total of 90 experiments.

3. Experimental Method

A direct gripping technique for UHMWPE fibers was used in this study as a result of problems associated with directly gluing fiber to cardboard substrates for experimentation. A tensile experiment using a glued fiber is rendered invalid if the fiber slips from the glue bond at any point during extension. A successful adhesive method applied to Dyneema SK76 depends upon the diameter of the fiber as noted by Hudspeth et al. (*5*), who successfully gripped 16-μm-diameter Dyneema fibers. Prior to using the direct gripping method described in this report, we used an optical microscope to hand-select fibers with a diameter of 14.5–16.9 μm, and used adhesive-based gripping methods to conduct 36 tensile experiments. None of the fibers from the 36 experiments were extended until failure; each sample slipped from the glue bond, rendering the experiment invalid. Searching through a yarn to identify a fiber that is small enough in diameter for tensile experiments is time-consuming, especially since the average fiber diameter is about 18.5 μm. Selecting fibers at random, we measured 276 fiber samples in this study, and found that only three had a diameter less than 16 μm. Based on the results of Hudspeth et al. (*5*), the upper limit of fiber diameter that may be gripped using adhesive methods alone is 16 μm,

though our results using adhesives suggests that this upper limit rests below a diameter of 14.5 μm. Based on this, adhesive methods do not work, and a direct gripping method is needed to characterize Dyneema SK76.

Using the direct gripping method, single fibers over a wide diameter range are clamped in a fixture that does not allow slippage. Fibers ranging in diameter from 14.5 to 22.3 μm were successfully gripped using this technique. One particularly large fiber sample with diameter of 35.9 ± 0.52 μm was successfully pulled to failure using the direct grip but was not included in the analysis due to its uncharacteristically large diameter. The specialized clamps used were designed to fit in both a quasi-static/intermediate rate experimental setup and a high-rate fiber–Split-Hopkinson tension bar (fiber-SHTB) setup. In the grip assembly, a single fiber mounted with cyanoacrylate glue on a cardboard specimen holder is inserted in the grip. The covers of the grip are tightened until the fiber is squeezed with enough force by the polycarbonate clamping blocks to ensure that the fiber will not slip out during the experiment. The cardboard supporting frame is then clipped away and removed by slipping the fiber out of the cyanoacrylate glue joint on the frame; this does not affect the gage area of the fiber that will be pulled in tension once the experiment begins. After removing the cardboard frame, the gage length of the fiber is carefully measured using a camera and calibrated dial indicator assembly.

A side view of the clamped grip and fiber is shown in figure 1a, while in figure 1b both grips are shown with a fiber spanning between them.

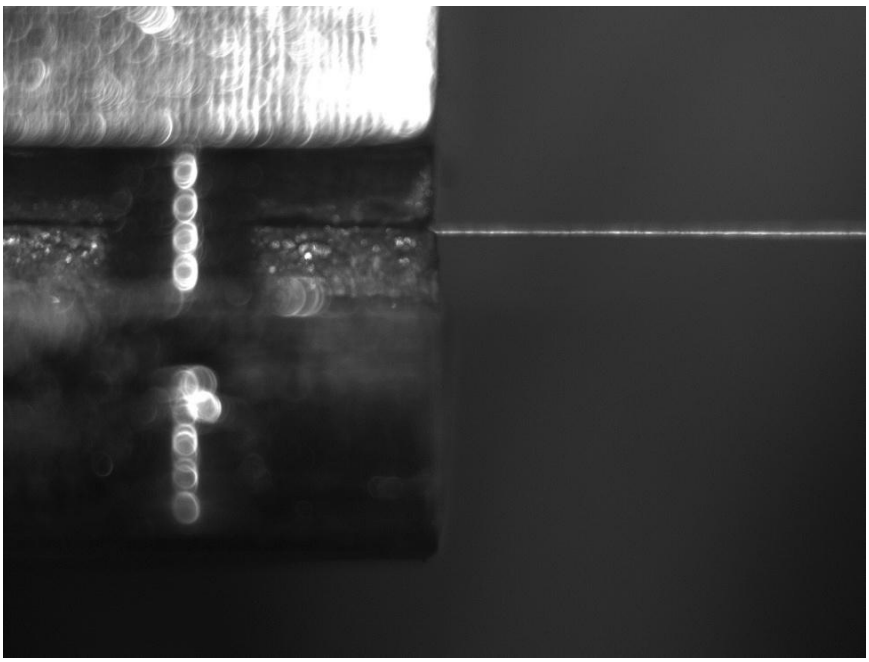

(a)

(b)

Figure 1. Left side of the gripping system (a) and gripping system with fiber clamped between the two grips (b).

The mechanical grips squeeze and deform the fiber to allow gripping to occur. A SEM image of the gripped area of a typical fiber sample is shown in figure 2 where the fiber was clamped in the grip and removed for imaging, and was not subjected to mechanical loading. From the images in figure 2, the sectional width of the fiber that has been deformed by the grip is noticeably larger

than the overall diameter of the nondeformed fiber. The original diameter of this fiber was 18.65 ± 0.4 μm, and after gripping, the ends of the fiber that have been squeezed by the grips are deformed to a width of approximately 54 μm. Using a constant volume assumption to estimate the resulting thickness of the deformed area, the gripped area of the fiber was deformed to a thickness of approximately 5–6 μm. If elastic compressibility was accounted for, the gripped thickness could be less than the estimated 5–6 μm.

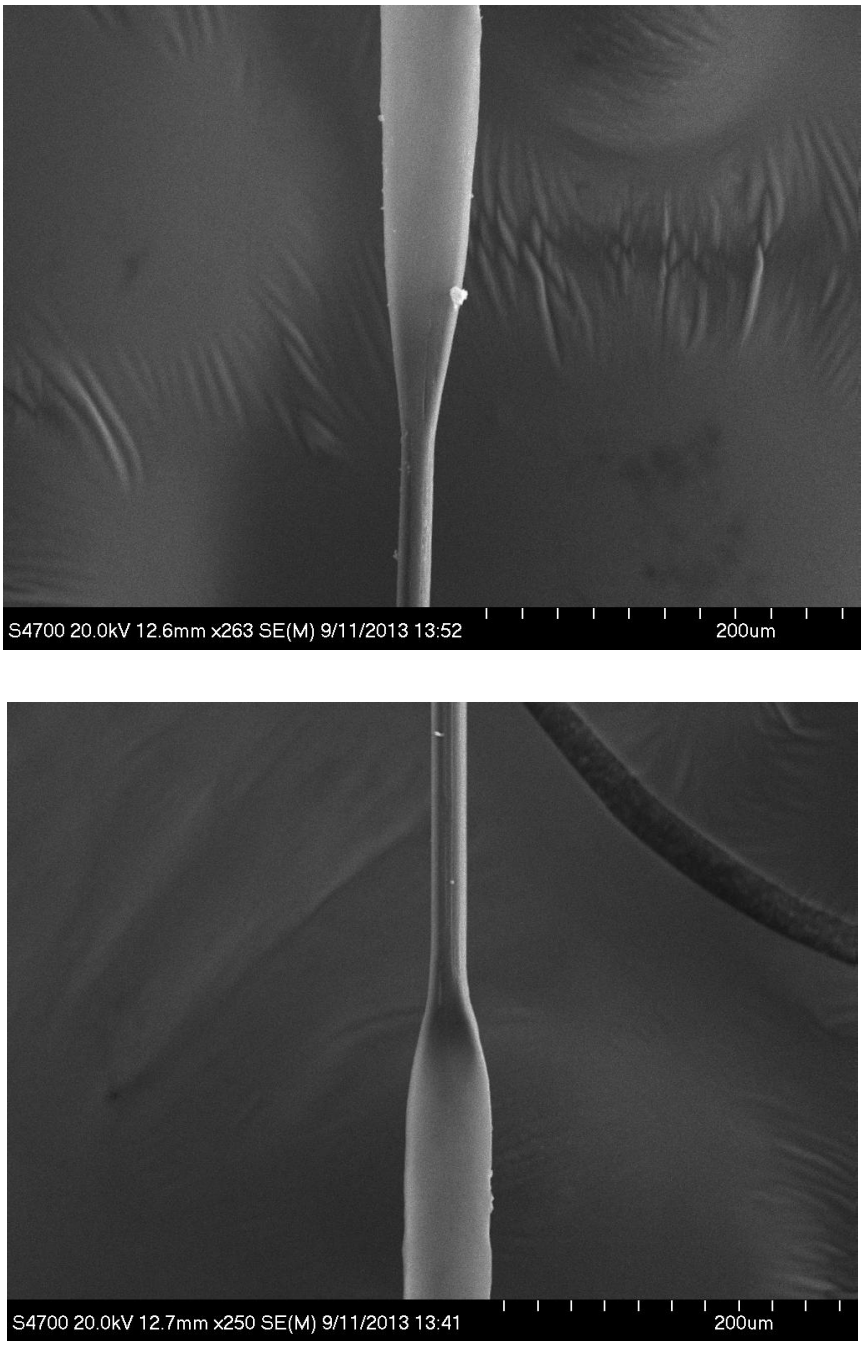

Figure 2. SEM images of the opposite ends of a fiber sample that has been clamped in the grips and removed for imaging.

3.1 Quasi-Static and Intermediate Rate Experiments

At quasi-static and intermediate rates of to 0.001 s^{-1} and 1 s^{-1}, a Bose Electroforce setup was used to evaluate the strength. The strain (ε) and strain rate ($\dot{\varepsilon}$) are calculated based on the gage length (l_s) of the sample:

$$\varepsilon = -\frac{d}{l_s} \tag{1}$$

$$\dot{\varepsilon} = -\frac{v}{l_s} \tag{2}$$

where d is the displacement of actuator and v is the velocity of the experiment. The specimen stress is calculated using

$$\sigma = \frac{P}{A_0} \tag{3}$$

where A_o is the initial cross-sectional area based upon the diameter measurement obtained using optical microscopy for each sample. Finally, P is the force measured by the load cell.

3.2 High-Rate Experiments

The high-rate behavior of the fiber was studied using a fiber-SHTB, a schematic of which is shown in figure 3. The fiber-SHTB is similar to the bar used by other authors (*5*, *10–13*, *17*), while the optical strain measurement is attributed to Lim et al. (*11*).

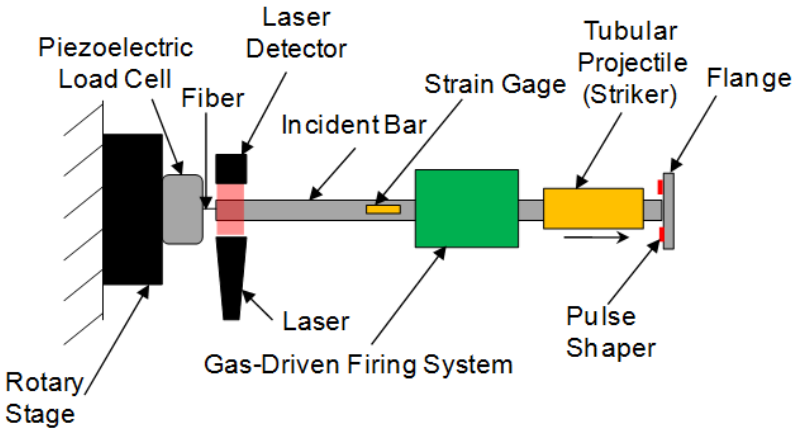

Figure 3. Schematic of fiber-SHTB.

Equations 1, 2, and 3 are used to obtain strain, strain rate, and stress in the high-rate experiment. The displacement measurement on the fiber-SHTB is obtained from the measured linear laser signal. Prior to the experiment, a displacement and voltage relation was obtained by uncovering the laser detector in set increments. The strain rate history is also obtained from differentiating the laser signal with respect to time.

4. Results and Discussion

4.1 Effectiveness of the Direct Gripping Technique

Overall, the direct gripping technique was successful at multiple gage lengths and strain rates. Representative stress-strain curves from a series of 5-mm-gage-length fibers tested at quasi-static strain rate are shown in figure 4. The stress-strain behavior in figure 4 shows that the fibers did not slip out of the grips during the experiments. A slipping fiber is characterized by a drop in load as the strain increases, followed by either an increase in load or a plateau in load as the strain continues to increase as the fiber slips from the glue, which is not depicted in figure 4. The load continues to increase with increasing strain until failure. In addition, failure stresses, failure strains, and overall stress-strain curve shape are similar to the results of Russell et al. (*3*) on SK76 single fibers, though a limited number of results were shown in that report.

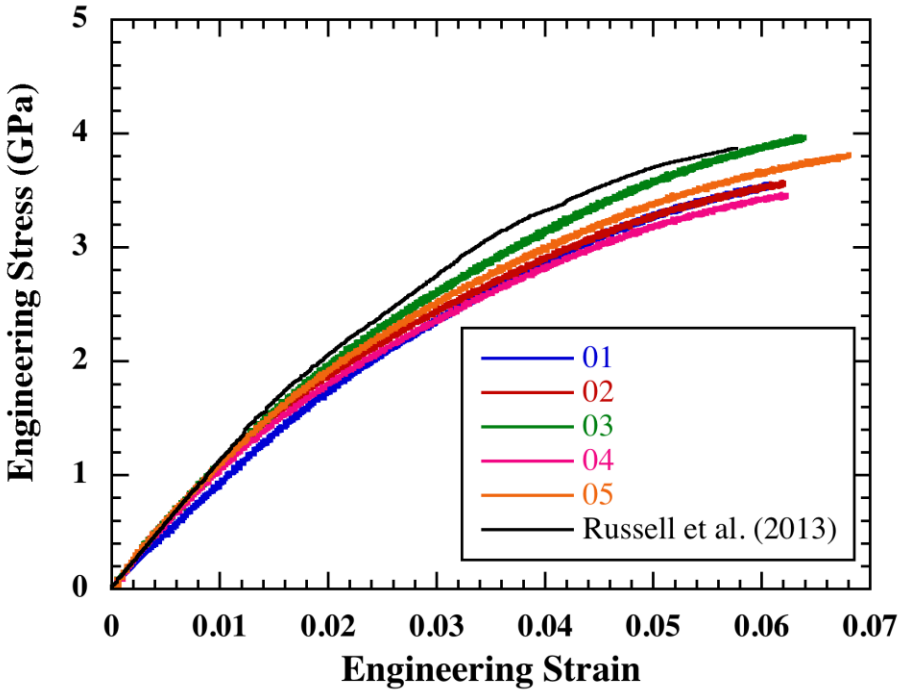

Figure 4. Typical stress-strain curves from quasi-static experiments including the results of Russell et al. (*3*).

The direct gripping method did not produce fractures or failures in the middle of the gage section 100% of the time. Different rates of success were experienced for different gage lengths and strain rates. A summary of the success rate for failure in the gage section at different experimental conditions is shown in table 1.

Table 1. Success rate of direct gripping method under different experimental conditions.

Gage Length (mm)	Quasi-Static Rate (%)	Intermediate Rate (%)	High Rate (%)
5	83	73	33
7	—	—	28
10	90	91	42
50	71	83	—

Note: Empty cells indicate that experiments were not conducted under those conditions.

As shown in table 1, experimental success was higher at quasi-static and intermediate rates than with high-rate experiments. Therefore, at high loading rates, more experiments must be conducted to obtain enough successful experiments to compare with experiments at lower loading rates. The success rate also does not appear to depend on the gage length. Table 2 shows a comparison of failures occurring in the gage section with failures at the grip in terms of failure strength. In all cases, fibers that failed at the grip had a weaker strength than those that failed in the gage section. At 5- and 7-mm gage lengths, the end-break fibers were about 7%–9% weaker, while at 10 mm, the end-break fibers were less than 1% weaker than the gage section failures. Previous low-rate studies on UHMWPE single fibers bonded directly to cardboard using epoxies show success rates as low as 10% (*2*) on 27.5-µm-diameter fibers. Prior to the present study using direct gripping, our attempts to study Dyneema fibers in the 14.5 to 16.9-µm-diameter range with adhesive gripping had a 0% success rate at all loading rates using adhesive methods.

Table 2. Comparison of gage section failures and failures at the grip at high rate.

High Rate	Failure in Gage Area	Failure at Fiber-Grip Interface	Ratio of Failure Strength at Grip Interface to Failure Strength in Gage Area (%)
Gage Length (mm)	Strength (GPa)	Strength (GPa)	
5	4.24 ± 0.39	3.86 ± 0.44	91.1
7	4.25 ± 0.21	3.99 ± 0.34	93.9
10	4.08 ± 0.17	4.07 ± 0.30	99.7

The gripping technique also works well at the high rate. Five typical high-rate stress-strain curves are shown in figure 5, which shows reasonable variation between experiments. There is no evidence of the fiber slipping out from the grips.

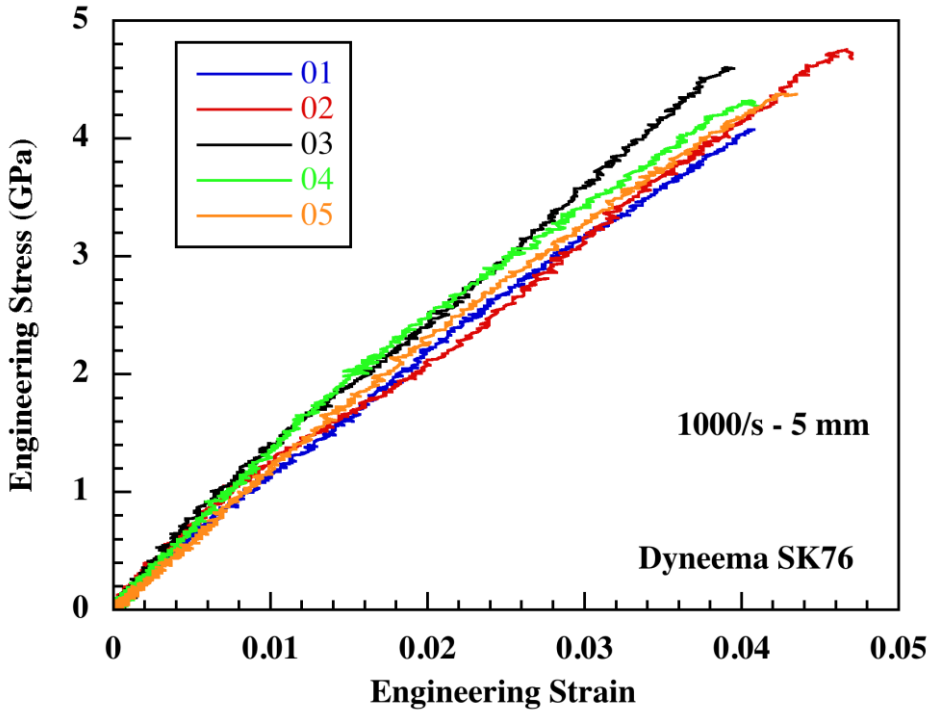

Figure 5. High-rate stress-strain curves for Dyneema SK76 with approximately 18-μm-diameter, 5-mm-gage-length samples.

4.2 Uniaxial Tensile Strength at Multiple Strain Rates

The strengths from uniaxial tension experiments conducted at various strain rates are shown in figure 6 as a function strain rate, and the values ±1 SD are given in table 3. In general, there is an increasing relationship between failure strength and strain rate, which has also been noted by other authors for UHMWPE (*3*, *5*, *6*, *18*, *19*).

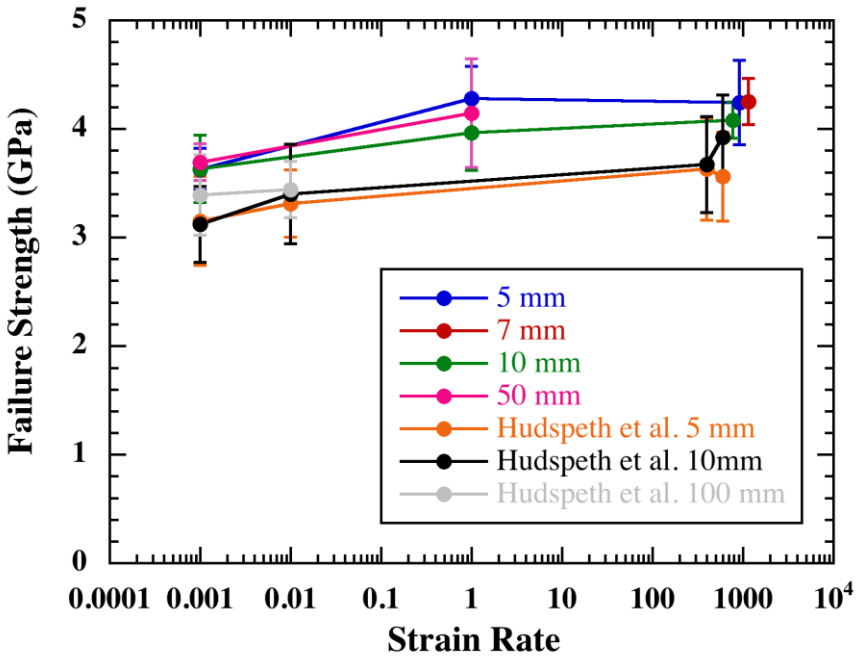

Figure 6. Effect of strain rate on the tensile strength for different gage lengths including the results of Hudspeth et al. (*5*).

Table 3. Averaged strengths ±1 SD at different strain rates and gage lengths.

Strain Rate (s^{-1})	5-mm Strength (GPa)	7-mm Strength (GPa)	10-mm Strength (GPa)	50-mm Strength (GPa)
0.001	3.63 ± 0.19	—	3.64 ± 0.31	3.69 ± 0.17
1.0	4.28 ± 0.30	—	3.96 ± 0.35	4.14 ± 0.50
775.0	—	—	4.08 ± 0.17	—
913.0	4.24 ± 0.39	—	—	—
1156.0	—	4.25 ± 0.21	—	—

In general, we found higher strengths than the results of Hudspeth et al. (*5*) for the Dyneema SK76 fibers. They found strengths of approximately 3.12–3.15 GPa for 5- and 10-mm gage lengths at 0.001 s^{-1}, with an increase to approximately 3.31–3.40 GPa at 0.01 s^{-1}, while we measured failure strengths of 3.63–3.69 GPa in the same range of strain rates. At high strain rates, Hudspeth et al. (*5*) noted strengths of 3.63–3.67 GPa for 5- and 10-mm gage lengths at 400 s^{-1}, while strengths of 3.56 and 3.92 GPa were measured for 5- and 10-mm gage length fibers, respectively, at 600 s^{-1}. At 1000 s^{-1}, our results show strengths of 4.08–4.25 GPa, which are notably higher than Hudspeth et al. Furthermore, the strengths from Hudspeth et al. show that long-gage-length fibers (100 mm) were stronger than short-gage-length (5- and 10-mm) fibers by about 8% at 0.001 s^{-1}. Our results do not show this difference when comparing the short (5- and

10-mm) gage-length fibers with the 50-mm-gage-length fibers. The average failure strength of the 5-, 10-, and 50-mm-gage-length fibers used in this study were 3.63 ± 0.19, 3.64 ± 0.31, and 3.69 ± 0.17 GPa, respectively, representing an increased failure strength of only 1.5% at the longer gage length. Unlike similar studies on Kevlar (*10–13*), we do not see the fiber strength increasing as the gage length decreases. Further studies on shorter gage length fibers would help probe the presence of any defects and also quantify the spacing of any strength increasing defects.

The results of failure strength suggest that Dyneema SK76 reaches a failure strength plateau at strain rates in the intermediate regime (1 s^{-1}), instead of increasing gradually from quasi-static to high rate as previous studies suggest (*5*), evidenced by the similarity of the strengths in the range of 1 s^{-1} and approximately 1000 s^{-1}. This plateau in strength at intermediate rate is similar to the behavior of Dyneema SK76 yarns observed by Russell et al. (*3*). In that study of yarn strength, the ultimate strength of Dyneema yarn reached a plateau just before a strain rate of 1 s^{-1}. In another study (*20*) of Dyneema SK60 single fibers, tensile strength at different temperatures was examined and related to strain rate, and the work to fracture was found to reach a constant value at a strain rate of approximately 1 s^{-1}. These results suggest that the plateau in failure strength reached at intermediate rate is a behavior independent of the fiber type and an inherent property of Dyneema fiber. Further studies on the tensile behavior extended to higher strain rates would confirm this finding.

4.3 Tensile Failure Strain at Multiple Strain Rates

The accepted method when conducting experiments on single fibers is that the failure strain must be corrected using the ASTM compliance correction method (*10–12*, *21*) even when experimentation is completed at high strain rates on a fiber-SHTB (*11*). Tables of the uncorrected and corrected failure strains using the method outlined in ASTM 1557-03 (*21*) are shown in tables 4 and 5, respectively. After the compliance correction is applied, the range of failure strain of the SK76 fiber becomes 2.58%–3.96%, which is close to the value of 3%–4% for similar fiber types (SK75 and SK78) as noted by the manufacturer (*7*). This gives greater confidence of the application of the direct gripping method applied to UHMWPE fibers.

Table 4. Uncorrected failure strains.

Strain Rate (s^{-1})	**5-mm Failure Strain (%)**	**7-mm Failure Strain (%)**	**10-mm Failure Strain (%)**	**50-mm Failure Strain (%)**
0.001	6.49 ± 0.43	—	5.53 ± 0.87	4.30 ± 0.38
1.0	5.70 ± 0.42	—	4.83 ± 0.72	3.6 ± 0.28
775.0	—	—	3.71 ± 0.26	—
913.0	4.11 ± 0.42	—	—	—
1156.0	—	4.52 ± 0.48	—	—

Table 5. ASTM 1557-03 compliance corrected failure strains.

Strain Rate (s^{-1})	5-mm Failure Strain (%)	7-mm Failure Strain (%)	10-mm Failure Strain (%)	50-mm Failure Strain (%)
0.001	3.48 ± 0.42	—	3.93 ± 0.96	3.96 ± 0.36
1.0	2.92 ± 0.23	—	3.35 ± 0.75	3.29 ± 0.25
775.0	—	—	3.00 ± 0.24	—
913.0	2.58 ± 0.31	—	—	—
1156.0	—	3.51 ± 0.57	—	—

Although ASTM 1557-03 (*21*) states that the fiber modulus must also be corrected through compliance correction, the data suggests this may not be accurate for Dyneema fiber. The ASTM 1557-03 standard assumes that the fiber response is linear until failure and corrects the modulus in a similar fashion. However, the stress-strain behavior at low and intermediate rates has a distinct concave downward shape (figures 4 and 8) due to creep, hence the initial modulus will not be the same as if the fiber was assumed to be linear until failure. For this reason, fiber modulus is not corrected using ASTM 1557-03.

4.4 Effect of Fiber Diameter on Failure Strength

Some studies have noted that restricting fiber diameter to within a certain range is necessary so that the fiber may be gripped using adhesives. This practice may lead to uncharacteristic failure strength values compared with strengths obtained through experimentation on fibers of a wider diameter range. In an effort to understand the effect of fiber diameter on failure strength at each gage length and strain rate, linear correlations (Pearson's r) were performed between the failure strength and fiber diameter with a significance of 0.05. A value of N=10 for each of the data sets gives a number of degrees of freedom of 8 (N–2 = 8). A typical plot of failure strength and fiber diameter is shown in figure 7. The full results of each of the gage length and strain rates are presented in table 6.

Based on the correlations shown in table 6, we find that three of the nine gage length and strain rate conditions exhibit statistically significant ($p < 0.05$) negative relationships exist between fiber diameter and failure strength. The variations of strength with diameter found in this study reinforce the need to conduct tensile strength experiments on a wide diameter range of UHMWPE single-fiber samples; the results shown in table 6 suggest that if only smaller diameter fibers are chosen for experimentation in some cases, the reported failure strengths may be higher than a study on fibers of a larger diameter range. Further studies that include larger sample sets would help elucidate the strength-diameter relationship found here.

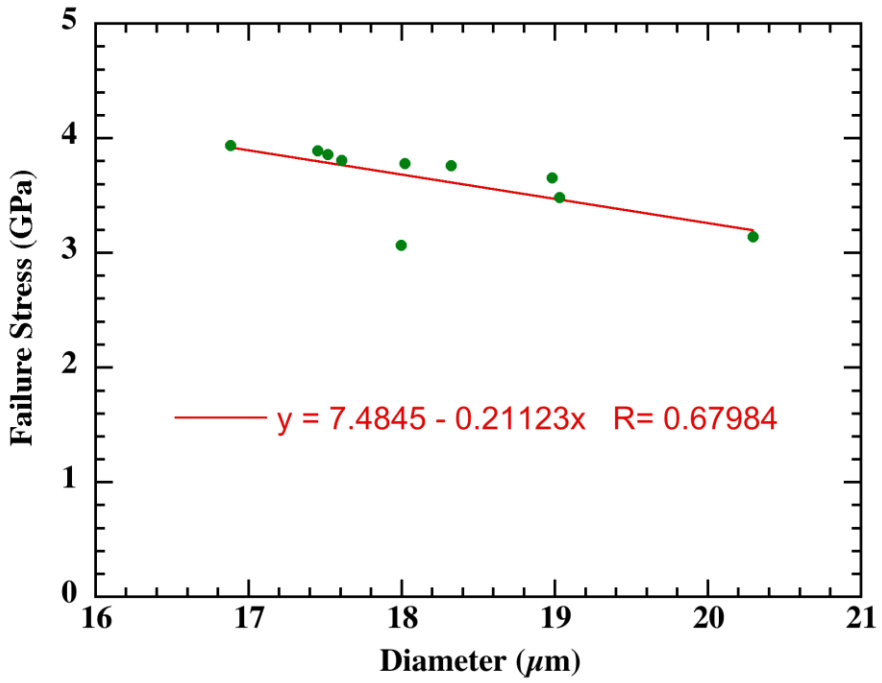

Figure 7. Dependence of failure strength on fiber diameter. This data set is from quasi-static loading rate with 10-mm-gage-length specimens.

Table 6. Correlation between failure strength and fiber diameter. Values of $p < 0.05$ are shaded, and represent a statistically significant negative relationship between diameter and failure strength.

Gage Length (mm)	Strain Rate (s^{-1})	Slope	Intercept	r(8)	p
5	0.001	–0.084	5.122	–0.535	0.111
10	0.001	–0.211	7.484	–0.680	0.031
50	0.001	0.007	3.567	0.043	0.906
5	1.0	–0.126	6.487	–0.589	0.073
10	1.0	–0.448	12.309	–0.656	0.043
50	1.0	–0.152	6.930	–0.295	0.407
5	1000.0	0.048	3.337	0.122	0.692
7	1000.0	–0.209	7.968	–0.711	0.032
10	1000.0	–0.106	5.988	–0.487	0.153

Based on the correlations shown in table 6, we find that three of the nine gage length and strain rate conditions exhibit statistically significant ($p < 0.05$) negative relationships between fiber diameter and failure strength. The variations of strength with diameter found in this study reinforce the need to conduct tensile strength experiments on a wide diameter range of UHMWPE single-fiber samples; the results shown in table 6 suggest that if only smaller

diameter fibers are chosen for experimentation in some cases, the reported failure strengths may be higher than a study on fibers of a larger diameter range. Further studies that include larger sample sets would help elucidate the strength-diameter relationship found here.

4.5 Shape of Stress-Strain Curves With Respect to Strain Rate

In general, the stress-strain behavior of UHMWPE fiber is increasingly linear with increasing strain rate (*3*, *6*, *9*). The average behavior of 5- and 10-mm-gage-length samples is shown in figure 8. The plots represent an average of 10 experiments, and error bars represent ±1 SD of strength at each strain value. At low rates, the primary deformation mode of UHMWPE fiber is creep (*3*, *22–25*), which was also specifically noted on nonballistic grades of Dyneema such as SK66 (*22*) and SK65 (*26*). In each case, the creep component increases with decreasing strain rate. The increase in linearity of the stress-strain curve is also seen when experiments at different temperatures are conducted (*22*), suggesting that the mechanism of failure at low temperatures is similar the mechanism of failure at high strain rates.

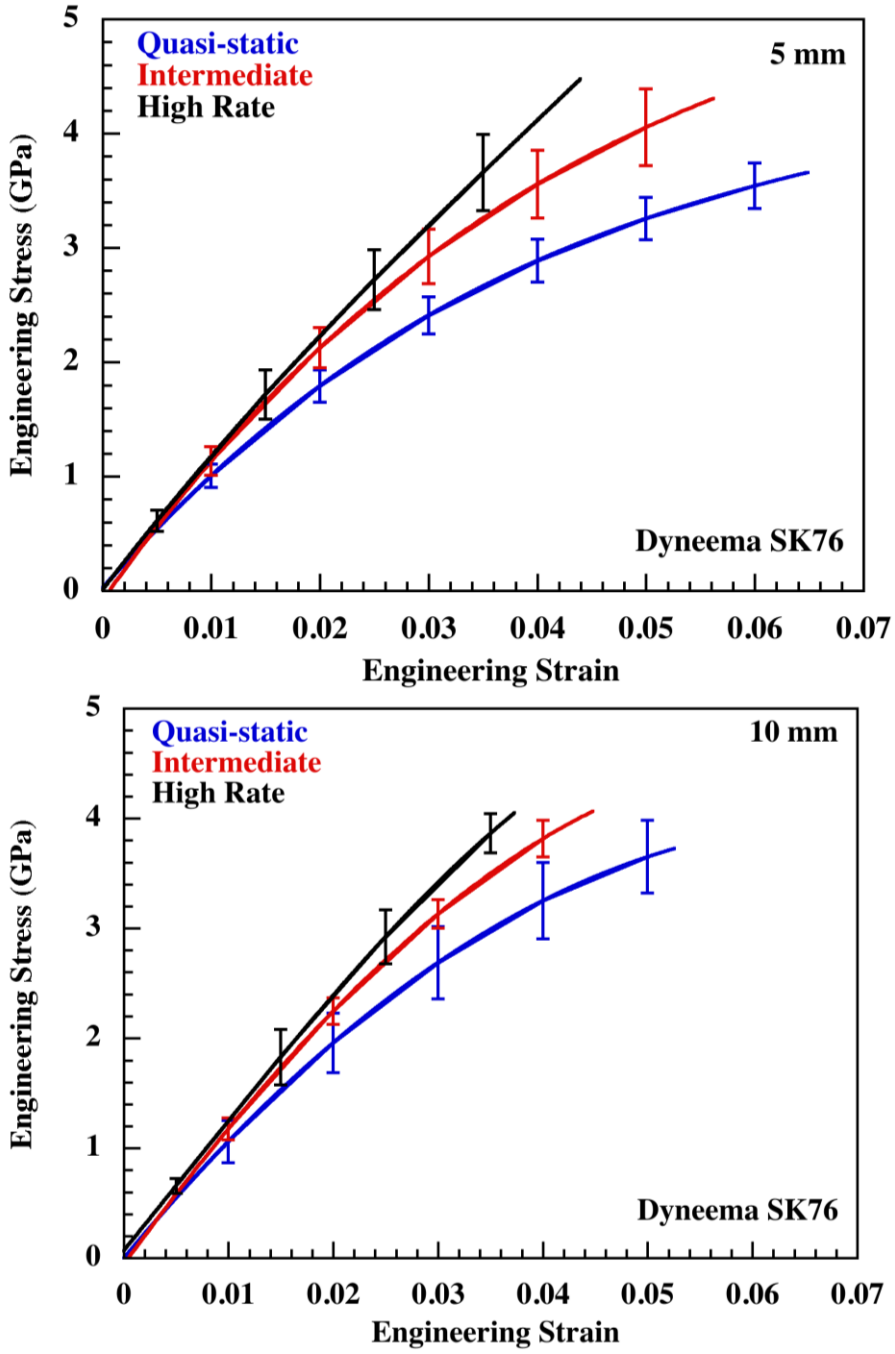

Figure 8. Stress-strain response at multiple strain rates. Note the increase in linearity for the same gage length with increasing strain rate. The curves in these plots represent the average behavior of 10 experiments.

5. Conclusions

Dyneema SK76 single fibers of diameter 18.22 ± 1.15 μm representing a range of 14.5–22.3 μm were successfully gripped and pulled in tension at strain rates of 0.001 s^{-1}, 1 s^{-1}, and approximately 1000 s^{-1} using a gripping technique that had not previously been applied to UHMWPE fibers. The gripping technique showed a high level of success at low and intermediate strain rates and a moderate level of success at high strain rates. Tensile strength of SK76 fiber increases with strain rate from low rate to intermediate (1 s^{-1}) rate, where a plateau in failure strength is reached at which there is no further increase in strength when the strain rate is increased to 1000 s^{-1}. The effect of defect distribution was studied by conducting experiments on fibers of multiple gage lengths ranging from 5 to 50 mm. The failure strength of the fiber did not depend on the gage length of the sample, indicating that the distribution of any critical defects in the fiber is at an effective spacing of less than 5 mm. With a sample size of 10, the linear dependence of fiber diameter on failure strength was found to have a statistically significant ($p < 0.05$) negative relationship for three of the nine investigated gage lengths and strain rates. Smaller diameter fibers attained higher failure stresses in these cases. More experiments are needed to further explore this finding.

The shape of the stress-strain curves for SK76 was similar to what other authors have found for UHMWPE fibers where the stress-strain curved increased in linearity with increasing strain rate. This was also noted by authors who investigated UHMWPE at different temperatures, suggesting that the mechanisms of deformation at low temperatures and high strain rates are similar. After the compliance of the experimental apparatus was accounted for by using multiple gage length samples at each rate, the effective failure strain of the Dyneema fiber was similar to manufacturer values for similar fiber types. These results can be used in single-fiber-based constitutive models for numerical simulation of impact events on soft armor.

6. References

1. Lin, S. P.; Han, J. L.; Yeh, J. T.; Chang, F. C.; Hsieh, K. H. Surface Modification and Physical Properties of Various UHMWPE Fiber Reinforced Modified Epoxy Composites. *Journal of Applied Polymer Science* **2007,** *104,* 655–665.
2. Umberger, P. D. Characterization and Response of Thermoplastic Composites and Constituents. Master's thesis, Virginia Polytechnic Institute and State University, Blacksburg, VA, 2010.
3. Russell, B. P; Karthikeyan, K.; Deshpande, V. S.; Fleck, N. A. The High Strain Rate Response of Ultra High Molecular Weight Polyethylene: From Fibre to Laminate. *International Journal of Impact Engineering* **2013,** *60,* 1–9.
4. Cochron, S.; Galvez, F.; Pintor, A.; Cendon, D.; Rosello, C.; Sanchez-Galvez, V. *Characterization of Fraglight Non-Woven Felt and Simulation of FSP's Impact In It;* R&D 8927-AN-01; Universidad Politecnica de Madrid (Spain) Escuela Tecnica Superior de Intenieros de Caminos, 2002; ADA408250.
5. Hudspeth, M.; Nie, X.; Chen, W. Dynamic Failure of Dyneema SK76 Single Fibers Under Biaxial Shear/Tension. *Polymer* **2012,** *53,* 5568–5574.
6. Cansfield, D.; Ward, I.; Woods, D.; Buckley, A.; Pierce J.; Wesley J. Tensile Strength of Ultra High Modulus Linear Polyethylene Filaments. *Polymer Communications* **1983,** *24,* 130–131.
7. Dyneema Comprehensive Fact Sheet; CIS YA100; DSM Dyneema LLC: Stanley, NC, January 2008. http://issuu.com/eurofibers/docs/name8f0d44 (accessed 10 June 2014).
8. *Spectra Fiber 900, 1000, and 2000;* AS-PF-PS9B; Allied Signal Inc. (now Honeywell): Morristown, NJ, 1999. http://www.honeywell-advancedfibersandcomposites.com /products/fibers/ (accessed 10 June 2014).
9. Schwartz, P.; Netravali, A.; Sembach, S. Effects of Strain Rate and Gauge Length on the Failure of Ultrahigh Strength Polyethylene. *Textile Research Journal* **1986,** *56* (8), 502–508.
10. Lim, J.; Zheng, J. Q.; Masters, K.; Chen, W. W. Mechanical Behavior of A265 Single Fibers. *Journal of Materials Science* **2010,** *45,* 652–661.
11. Lim, J.; Chen, W. W.; Zheng J. Q. Dynamic Small Strain Measurements of Kevlar 129 Single Fibers With a Miniaturized Tension Kolsky Bar. *Polymer Testing* **2010,** *29,* 701–705.
12. Lim, J.; Zheng, J. Q.; Masters, K.; Chen, W. W. Effects of Gage Length Loading Rates and Damage on the Strength of PPTA Fibers. *International Journal of Impact Engineering* **2011,** *38,* 219–227.

13. Sanborn, B.; Weerasooriya, T. *Quantifying Damage at Multiple Loading Rates to Kevlar KM2 Fibers Due to Weaving and Finishing;* ARL-TR-6465; U.S. Army Research Laboratory: Aberdeen Proving Ground, MD, June 2013.

14. Kim, J. H.; Heckert, A. N.; Leigh, S. D.; Rhorer, R. L.; Kobayashi, H; McDonough, W. G.; Rice, K. D.; Holmes, G. A. Statistical Analysis of PPTA Fiber Strengths Measured Under High Strain Rate Condition. *Composites Science and Technology* **2014,** *98,* 93–99.

15. Kim, J. H.; Heckert, N. A.; McDonough, W. G.; Rice, K. D.; Holmes, G. A. Single Fiber Tensile Properties Measured by the Kolsky Bar Using a Direct Fiber Clamping Method. In *Proceedings of Society for Experimental Mechanics Conference*, Lombard, IL, 3–5 June 2013.

16. Kim, J. H.; Heckert, N. A.; Leigh, S. D.; Kobayashi, H.; McDonough, W. G.; Rice, K. D.; Holmes, G. A. Effects of Fiber Gripping Methods on the Single Fiber Tensile Test: I. Non-Parametric Statistical Analysis. *Journal of Materials Science* **2013,** *48,* 3623–3673.

17. Cheng, M.; Chen, W.; Weerasooriya, T. Mechanical Properties of Kevlar KM2 Single Fiber. *Journal of Engineering Materials and Technology* **2005,** *127,* 197–203.

18. Prevorsek, D; Chin, H.; Kwon, Y.; Field, J. Strain Rate Effects in Ultrastrong Polyethylene Fibers and Composites. *Proceedings of the Fiber Society 50th Anniversary Technical Conference,* Princeton, New Jersey, 1991; Vol. 47, pp 45–66.

19. Wagner, H. D.; Aronhime, J.; Marom, G. Dependence of the Tensile Strength of Pitch-Based Carbon and Para-Aramid Fibres on the Rate of Strain. *Proceedings of the Royal Society of London Series A, Mathematical and Physical Sciences* **1990,** *428* (1875), 493–510.

20. Govaert, L. E.; Peijs, T. Tensile Strength and Work of Fracture of Oriented Polyethylene Fibre. *Polymer* **1995,** *36* (23), 4425–4431.

21. ASTM-C1557-03. Standard Test Method for Tensile Strength and Young's Modulus of Fibers. *Annu. Book ASTM Stand*. **2008**.

22. Govaert, L. E.; Bastiaansen, C. W. M.; Leblans, P. J. R. Stress-Strain Analysis of Oriented Polyethylene. *Polymer* **1993,** *34* (3), 534–540.

23. Wilding, M. A.; Ward, I. M. Tensile Creep and Recovery in Ultra-High Modulus Linear Polyethylenes. *Polymer* **1978,** *19,* 969–976.

24. Wilding, M. A.; Ward, I. M. Creep and Recovery in Ultra-High Modulus Polyethylene. *Polymer* **1978,** *22,* 870–876.

25. Wilding, M. A.; Ward, I. M. Creep and Stress-Relaxation in Ultra-High Modulus Linear Polyethylene. *Journal of Materials Science* **1984,** *19,* 629–636.

26. Liu, X.; Yu, W. Evaluation of the Tensile Properties and Thermal Stability of Ultrahigh-Molecular-Weight Polyethylene Fibers. *Journal of Applied Polymer Science* **2005,** *97*, 310–315.

1 (PDF) DEFENSE TECHNICAL INFORMATION CTR DTIC OCA

2 (PDF) DIR USARL IMAL HRA RDRL CIO LL

1 (PDF) GOVT PRINTG OFC A MALHOTRA

1 (PDF) US ARMY ATC TEDT AT SLB A FOURNIER

1 (PDF) PURDUE UNIV DEPT OF AERONAUTICS & ASTRONAUTICS W CHEN

1 (PDF) UNIV OF NORTH TEXAS DEPT OF MECHL & ENERGY ENGRNG X NIE

2 (PDF) MASSACHUSETTS INST OF TECHLGY INST FOR SOLDIER NANOTECHNOLOGIES R RADOVITZKY S SOCRATE

1 (PDF) HUMAN SYSTEMS DEPT NVL AIR WARFARE CTR AIRCRAFT DIV B SHENDER

2 (PDF) DEPT OF MECHL ENGRNG THE JOHNS HOPKINS UNIV LATROBE 122 K T RAMESH V NGUYEN

1 (PDF) UNIV OF TEXAS AUSTIN AEROSPACE ENGRNG AND ENGRNG MECHS K RAVI-CHANDAR

2 (PDF) JTAPIC PROG OFC US ARMY MEDICAL RSRCH AND MTRL CMND MRMC RTB J USCILOWICZ F LEBEDA

1 (PDF) NVL SURFACE WARFARE CTR CODE 664 P DUDT

1 (PDF) TARDEC RDTA RS R SCHERER

1 (PDF) NATICK SOLDIER RSRCH DEV AND ENGRNG CTR NSRDEC AMSRD NSC WS TB M G CARBONI

6 (PDF) NATICK SOLDIER RSRCH DEV AND ENGRNG CTR NSRDEC RDNS D M CODEGA RDNS WPW P R DILALLA RNDS TSM M STATKUS RDNS WSD B J WARD P CUNNIFF M MAFFEO

2 (PDF) SOUTHWEST RSRCH INST MECHL AND MTRLS ENGRG DIV MTRLS ENGRG DEPT D NICOLELLA W FRANCIS

1 (PDF) SANDIA NATL LABS B SONG

1 (PDF) THE UNIV OF UTAH K L MONSON

1 (PDF) COLUMBIA UNIV 351 ENGINEERING TERRACE B MORRISON

1 (PDF) APPLIED RSRCH ASSOC INC SOUTHWEST DIV C E NEEDHAM

2 (PDF) CTR FOR INJURY BIOMECHANICS WAKE FOREST UNIV J STITZEL F S GAYZIK

1 (PDF) US INFANTRY CTR
MTRLS LOG NCO SCI TECHNLGY ADVISOR
SOLDIER DIV
S VAKERICS

3 (PDF) NATL GROUND INTLLGNC CTR
D EPPERLY
T SHAVER
T WATERBURY

2 (PDF) PROG EXECUTIVE OFC SOLDIER
K MASTERS
J ZHENG

2 (PDF) SOUTHWEST RSRCH INST
T HOLMQUIST
G JOHNSON

1 (PDF) AIR FORCE RSRCH LAB
AFRL RWMW
B MARTIN

101 (PDF) DIR USARL
RDRL HRS C
W HAIRSTON
B LANCE
K MCDOWELL
K OIE
J VETTEL
RDRL ROE M
D STEPP
RDRL ROE V
L RUSSELL
RDRL SL
R COATES
RDRL SLB A
B WARD
RDRL SLB W
A BREUER
N EBERIUS
P GILLICH
C KENNEDY
A KULAGA
W MERMAGEN
K RAFAELS
R SPINK
RDRL WM
P BAKER
B FORCH
S KARNA
J MCCAULEY
P PLOSTINS
RDRL WML
J NEWILL
M ZOLTOSKI
RDRL WML A
W OBERLE
J SOUTH
RDRL WML G
G BROWN
RDRL WML H
T EHLERS
M FERMEN-COKER
L MAGNESS
C MEYER
D SCHEFFLER
S SCHRAML
B SCHUSTER
RDRL WMM
J BEATTY
B DOWDING
RDRL WMM A
D O'BRIEN
E WETZEL
RDRL WMM B
A BUJANDA
B CHEESEMAN
G GAZONAS
B LOVE
P MOY
C RANDOW
M VANLANDINGHAM
C YEN
RDRL WMM C
R JENSEN
J LA SCALA
RDRL WMM D
R CARTER
E CHIN
S WALSH
W ZIGLER
RDRL WMM E
G GILDE
J LASALVIA
P PATEL
J SINGH
J SWAB
RDRL WMM F
S GRENDAHL
E KLIER
L KECSKES
RDRL WMM G
J LENHART
R MROZEK
A RAWLETT
K STRAWHECKER
RDRL WMP
S SCHOENFELD

RDRL WMP B
A DAGRO
A DWIVEDI
A GUNNARSSON
C HOPPEL
M LYNCH
D POWELL
B SANBORN
S SATAPATHY
M SCHEIDLER
T WEERASOORIYA
RDRL WMP C
R BECKER
S BILYK
T BJERKE
J BRADLEY
D CASEM
J CLAYTON
D DANDEKAR
M GREENFIELD
B LEAVY
C MEREDITH
M RAFTENBERG
C WILLIAMS
RDRL WMP D
R DONEY
D KLEPONIS
J RUNYEON
B SCOTT
B VONK
RDRL WMP E
S BARTUS
M BURKINS
D HACKBARTH
RDRL WMP F
A FRYDMAN
E FIORAVANTE
N GNIAZDOWSKI
R GUPTA
R KARGUS
RDRL WMP G
N ELDREDGE

4 DRDC VALCARTIER
(PDF) K WILLIAMS
A BOUAMOUL
L MARTINEAU
D NANDLALL

1 DRDC TORONTO
(PDF) C BURRELL

1 HUMAN PROTECTION AND
(PDF) PERFORM DIV
DEFENCE SCI AND TECHLGY ORGN
DEPT OF DEFENCE
T RADTKE

1 DEFENCE SCI AND TECHLGY ORGN
(PDF) S WECKERT